Thermochimica Acta 492 (2009) 37–44

Contents lists available at ScienceDirect

Thermochimica Acta

journal homepage: www.elsevier.com/locate/tca

Dynamic and apparent specific heats during transformation of water in partly filled nanopores during slow cooling to 110 K and heating

E. Tombari [a], C. Ferrari [a], G. Salvetti [a], G.P. Johari [b,*]

[a] Istituto per i Processi Chimico-Fisici del CNR, via G. Moruzzi 1, 56124 Pisa, Italy
[b] Department of Materials Science and Engineering, McMaster University, Hamilton, Ontario L8S 4L7, Canada

ARTICLE INFO

Article history:
Available online 18 May 2009

Keywords:
Water
Vycor
Nanoconfinement
Specific heat
Ice
Crystallization and melting

ABSTRACT

The specific heat of water in partially and completely filled 4 nm pores of Vycor has been studied by static and dynamic calorimetry. Water was transferred to the pores in controlled amounts of 4.4–22 wt% (i.e., 20–100% filling of pores) isothermally *via* the vapour phase in a closed system, and measurements were made on cooling from 280 to 110 K at 12 K/h and thereafter on heating from 110 K at the same rate. On cooling, a marginally small exothermic peak appeared at ~233 K for 20% filling, and the peak grew in intensity with more water in the pores. But it vanished for 100% filling. For 46 and 100% filling of the pores, a sharp crystallization peak appeared at ~250 K. On heating from 110 K, a broad endothermic peak appeared for all samples, the peak became narrower with increase in the pore-filling and its onset temperature increased. The effect also appeared in the dynamic specific heat but was less pronounced. We envisage that in partially filled pores, H_2O molecules form bulkier clusters attached to the silica wall. The crystallization peak is at ~233 K and the melting peak at 255 K. The H_2O clusters grow with increase in filling, but vanish for 100% filling. For 46% filling some regions of the pores also contain closely packed H_2O that crystallize at 248 K and melt at ~260 K (all references to peak). Water in 100% filled pores crystallizes at 250 K and the solid melts at 260 K. Crystallization of 46% filled sample over different T ranges showed broadened endotherm on heating, which was due to merging of two peaks from two-step melting. The rise in the onset temperature and the narrowing of the endotherm with increase in the pore water, are remarkably similar to those observed on increasing the size of 100% filled pores. It is necessary to use both cooling and heating to reveal the structural transformations in nanopores.

1. Introduction

Water in nanopores differs structurally from bulk water. Nevertheless, studies of nanoconfined supercooled water are performed with an expectation that it would help in revealing the behaviour of bulk supercooled water in its unaccessible temperature range. An article [1] by one of us in this journal-issue has already described some of these features and limitations of the concept. Briefly, in amorphous silica pores, water molecules form hydrogen bonds with the siloxane group on the pore-wall forming a layer or nanoshell attached to the pore-wall. On cooling, this layer does not crystallize while most of the remaining water crystallizes. Diffractions studies have shown that crystallization of pore water occurs to different types of ices on cooling, and in some cases the state of water reorganizes to a lower entropy, undefined structure. On heating, the ices melt and the structure reverts to the high entropy state gradually with changing T. In pores of diameter larger than ~2 nm, water has been found to crystallize to cubic ice, hexagonal ice or their mixture, and in pores of diameter smaller than 2 nm, water does not apparently crystallize. In most studies of confined water at temperatures below 200 K, the crystalline solid is found to coexist with the melt or with an otherwise disordered structure. Diffraction studies have shown that in some silica nanopores distorted or defective lattice structure of the ices are formed [2–5].

More recently, it has been found that (i) freezing and melting in pores larger than 3 nm occurs over a wide temperature range, with a considerable hysteresis on cooling and heating [6–11], (ii) an ice–water equilibrium [8,12] persists over a certain temperature range, (iii) the energy of an H_2O molecule varies with both its position in a nanopore [13] and the amount of water [7,13,14] in the pore, and (iv) C_p of nanoconfined water is higher than that of the bulk water and decreases to the bulk water value when pores are completely filled [14]. In the last two studies the amount of water that entered the 4 nm diameter (size) pores of Vycor *via* the vapour phase was controlled between 8.3 and 100% filling by providing a water droplet of known mass separated from the Vycor by an air gap inside a sealed container. The container was inserted in the calorimeter and the heat released as well as C_p during the spon-

* Corresponding author. Tel.: +1 905 525 9140x24941; fax: +1 905 528 9295.
E-mail address: joharig@mcmaster.ca (G.P. Johari).

0040-6031/$ – see front matter © 2009 Elsevier B.V. All rights reserved.
doi:10.1016/j.tca.2009.05.001

taneous transfer of water from bulk to nanopores was measured in real time. Thermodynamics and crystallization of water in the 100% filled 4 nm pores of Vycor has also been studied during cooling to 240 K and thereafter on heating [7]. Those studies showed that hydrogen bonding in nanoconfined water not only differs from that in bulk water but also it varies with the pore size and the extent of pore-filling.

It is also known that both the crystallization of confined water on cooling and melting of the crystals formed on heating vary with the size of the completely filled pores. Since the extent of hydrogen bonding is expected to vary with the amount of water in the pores of a given size, and this has relevance to a host of biological and physical processes in nature, we performed a detailed study of transformation of water in partially filled 4 nm diameter pores in Vycor. Here, we report a study of C_p as the water in partially filled pores froze or vitrifed during cooling from 280 to 110 K, and thereafter as the frozen state transformed during heating to 280 K. We used both the usual calorimetry and dynamic calorimetry for the study, with extremely slow cooling and heating rates of 12 K/h. Thus, thermodynamic equilibrium was achieved at much lower temperatures than in the 10 K/min heating rate in the usual DSC measurements. We investigate the change in the thermal effects when the pore-filling is gradually increased from 20 to 100%, and compare the results against those observed for 100% filled pores of increasing size in other nanoporous solids.

2. Experimental methods

The equipment and measurement technique are similar to those described in studies performed at temperatures above 235 K [15]. A new cold bath was constructed such that the calorimetric head could be immersed in its liquid nitrogen reservoir and dry nitrogen gas was used for circulation in the system to prevent moisture condensation. The details of the design will be published elsewhere. Calibration for the temperature scale was performed by using the (two) phase transition temperatures of cyclopentane and the melting point of water. Calibration for heat flow was performed by using benzoic acid as standard for specific heat. Although, only apparent heat capacity, $C_{p,\mathrm{app}}$, data were needed for our investigations, we also measured the real and imaginary components of the complex specific heat, C_p' and C_p'', by temperature modulation at 3.3 mHz frequency with peak to peak amplitude of 1 K for temperature modulation. Here, $C_{p,\mathrm{app}}$ refers to the usual specific heat measured in a DSC experiment in which it is time dependent in the glass transition region and in the glassy state, and C_p' and C_p'' refer, respectively, to the real and imaginary components of the complex specific heat, $C_p^* = C_p' + iC_p''$, where $i = \sqrt{-1}$ in both standard and quasi-isothermal measurements. The quantity C_p' is also referred to as reversible part of the specific heat. For more information and relations between $C_{p,\mathrm{app}}$, C_p' and C_p'' see Ref. [16]. The dynamic calorimetry was performed by superposing a temperature modulation to the normal temperature scanning calorimetry. This has a special advantage because the data obtained have higher signal to noise ratio than the data obtained in normal scanning calorimetry. It was also necessary in those cases in which the samples contained low amount of water and, consequently, the difference between $C_{p,\mathrm{app}}$ of the sample and of that of the dry Vycor was relatively small. The baseline in dynamic calorimetry was found to be more stable and for a longer period than in normal calorimetry. For both $C_{p,\mathrm{app}}$ and C_p', the data obtained during repeated heating and cooling were within the experimental reproducibility of 2%.

Water of reagent grade purchased from Angelini SpA was used. Cylindrical rods of Vycor 7930 in 6 mm length, 2 mm diameter and ~29 mg in weight were purchased from Corning, USA. Its composition is 96% SiO_2, 3% B_2O_3, 0.04% Na_2O and <1% ($Al_2O_3 + ZrO_2$), and in the dry state, its density = 1.5 g/cm^3, void space = 28% by volume, internal surface area = 250 m^2/g, average pore diameter (size) = 4 nm, and OH surface density of about 7 OH/nm^2. The rods were cleaned with distilled water and heated to 413 K for 12 h, dehydrated by keeping on silica gel for 24 h and kept stored in a desiccator prior to use. Thermogravimetric analysis performed after heating the rods showed no change in the mass [7]. The interconnected channels of 4 nm average diameter have a distribution of shapes and sizes, and nitrogen desorption studies of porous silica gel glass with nominally 15–30 nm diameter (size) pores have shown a distribution of pore size [11] but for Vycor 7930 this distribution is relatively narrow. The channels (pores) and some of multi-channel junctions terminate on the surface.

We used the manufacturer's data on the pore volume, surface area and density to calculate the amount of water per g of dry Vycor needed to fill its 4 nm pores. It was 19–22 wt%. As in our previous studies [13,14] we used samples of Vycor containing 4.4, 5.9, 7.7, 10 and 22 wt% water (= mass of water × 100/mass of dry Vycor). These amounts correspond, respectively, to 20, 27, 35, 46 and 100% filling of the 4 nm pores. The procedure for incorporating the desired amount of water in dry Vycor has been described earlier [13,14]. Briefly, a cleaned and dried 90 mm long pyrex tube of 2.2 mm internal diameter, and 0.3 mm wall thickness was used as the sample holder, which acted as an assembly that was inserted in the calorimeter. The required amount of water for transfer to Vycor *via* the vapour route was syringed into the tube's closed end. It was frozen to ice by vertically keeping the tube immersed in a bath at 250 K. The tube was then kept horizontally and eight pre-cleaned and weighed (nominally 235 mg) dry Vycor rods were inserted and kept close to the open end of the tube, thus providing an air space between the water and the Vycor rods. The tube was hermetically sealed by fusing with a miniature flame, brought to room temperature, which melted the ice and the water remained confined to one end of the tube by surface tension forces. The assembly of this closed system was inserted horizontally in the calorimeter cell maintained at 358 K, a temperature at which the air space separating water from Vycor was at a water saturation pressure. The H_2O molecules thus entered the nanopores *via* the vapour phase at saturation pressure. The transfer of bulk water to nanopores in this closed system occurred in two stages. First, nanopores on Vycor's surface were nearly filled at a certain rate as long as bulk water in the sample holder was available to maintain saturation pressure. Thereafter, a redistribution of water in the pores occurred by diffusion of H_2O in the pores. The samples in the sealed state were kept for long enough time to allow all the water to transfer uniformly in the 4 nm pores of Vycor, as described elsewhere [13,14]. In a typical procedure, the sample was kept at 280 K for 1 h, cooled to 110 K at 12 K/h rate, kept at 110 K for 1 h and then finally heated to 280 K at 12 K/h rate, and $C_{p,\mathrm{app}}$, C_p' and C_p'' were measured throughout this period.

Over most of the temperature range of the study, molecular relaxation time of water and ice is much shorter than the 300 s time scale of 3.3 mHz frequency used here. Therefore, C_p'' is expected to remain zero and only C_p' is expected to vary with T. Nevertheless, both C_p' and C_p'' were measured. As found in most experiments in which a first order transition occurs, C_p' and C_p'' were greatly effected by the rapidity of the heat released or absorbed during the transition. The C_p'' data are ignored here and only the C_p' data are reported. This C_p' therefore contains the effect of change in the equilibrium and vibrational C_p with T, the contributions of the thermally reversible transformation processes [16] and any artefact from loss of stationery state when the heat released or absorbed with changing T is too rapid [17]. In the temperature range where this transformation was absent or negligible, C_p'' was negligibly small. Since the opposite signs of the rates of cooling and heating have been ignored, the exothermic and endothermic peaks in $C_{p,\mathrm{app}}$ appear in the same positive direction.

3. Results

Fig. 1 shows the plots of $C_{p,app}$ and C'_p for water in 4 nm pores of Vycor containing 4.4, 5.9, 7.7, 10, and 22 wt% water (20, 27, 35, 46 and 100% filling of the pores). The samples were cooled at 12 K/h from 280 to 110 K. For clarity, the plots have been shifted upwards and the scale-shift and the amount of water in wt% and percentage filling are noted. On cooling, the 4.4 wt% pore water shows a very small peak at ~233 K. This peak grows until 10 wt% and vanishes for 22 wt% pore water. A new small peak at 243 K and a large sharp peak at 247 K appear for the 10 wt% pore water and both become larger for the 22 wt% pore water. Corresponding features appear in the C'_p plot, but with greatly reduced intensity. Large exothermic effects at T near 250 K are due to crystallization of supercooled water. Since the transformation is fast, the heat effect changes rapidly with T, and stationary conditions needed for determining C'_p cease to exist. Thus, the measured C'_p shows a large scatter.

Fig. 2 shows the corresponding plots obtained on heating the five samples from 110 to 280 K. Because of the large magnitude of errors in the baseline stability relative to the signal amplitude from the transformation of the sample, the $C_{p,app}$ data for 4.4 wt% pore water are excluded here. A broad peak appears at ~250 K for 5.9 wt% pore water, which becomes larger as the amount of water is increased and the peak shifts ultimately to 260 K for 22 wt% pore water. The peak appears as an overlap of two peaks, one of which, of small intensity, appears as low temperature shoulder that is clearly notable for the 10 wt% pore water. Corresponding features appear in the C'_p plot, but with greatly reduced intensity.

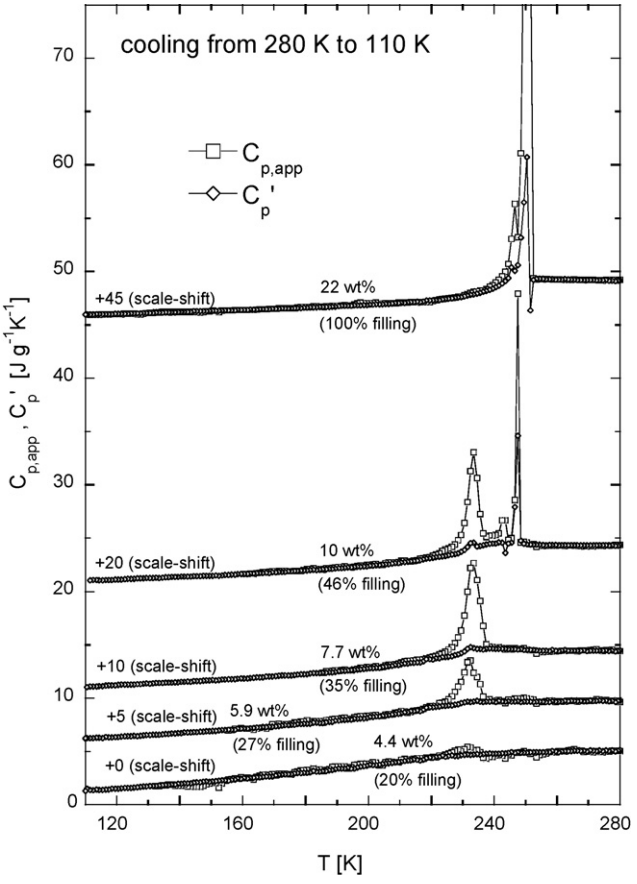

Fig. 1. The plots of $C_{p,app}$ and C'_p for water in 4 nm pores of Vycor containing 4.4, 5.9, 7.7, 10 and 22 wt% water (20, 27, 35, 46 and 100% pore-filling). Measurements made during cooling the samples at 12 K/h from 280 to 110 K. The plots have been shifted upwards and the scale-shift is noted.

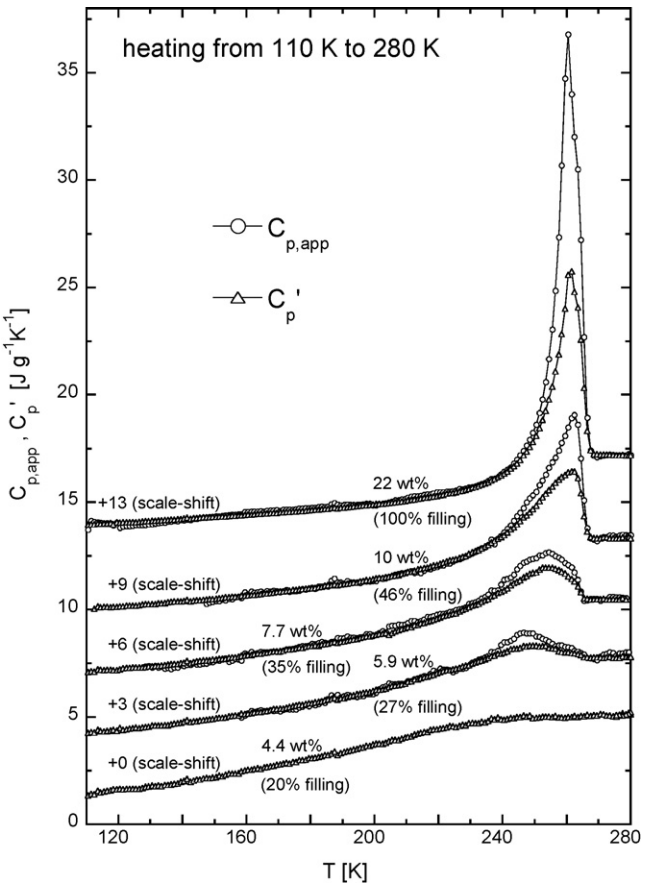

Fig. 2. The plots of $C_{p,app}$ and C'_p for water in 4 nm pores of Vycor containing 4.4, 5.9, 7.7, 10 and 22 wt% water (20, 27, 35, 46 and 100% pore-filling). Measurements made during heating at 12 K/h from 110 to 280 K after the precooled samples had been kept at 110 K for 1 h. The plots have been shifted upwards and the scale-shift is noted.

For comparison between $C_{p,app}$ measured during cooling and during heating, we have cross-plotted the data from Figs. 1 and 2 in Fig. 3. The plots show that the features observed on cooling do not appear on heating. There is a considerable hysteresis in the temperature of the peaks as well as of $C_{p,app}$ at a given T. For showing the difference between C'_p measured during cooling and heating, we have cross-plotted also the C'_p data in Fig. 4. Here, the data for 4.4 wt% pore water are the same for cooling and heating except near 245 K, as is evident in the insert of Fig. 4. The difference is more evident in the data for 5.9 wt% pore water and it increases with increase in the amount of pore water, reaching a maximum for 22 wt% pore water.

Calorimetric behaviour of water has been studied as a function of pore-filling in several earlier studies. Bellissent-Funel et al [18] studied water in two sets of partially filled pores of Vycor 7930 also, but the average pore size given by them is 5 nm. In one study, Vycor was fully hydrated (24.5% water) and in the other it was 56% hydrated (13.6% water). They found that while two exothermic peaks appear on cooling the 100% filled pores at 2 K/min rate and two endothermic peaks on heating, for partially filled pores only one exothermic peak appeared for freezing and only one endothermic peak on melting. The exothermic peak was shifted by ~2 K to a lower T. For water in the 100% filled pores, the first exotherm in the 263–255 K was attributed to "extra pore water" and the two melting endotherms to two phase melting.

Zanotti et al. [19] also studied 25% hydrated Vycor 7930, they found an apparent first order transition with two overlapping sharp

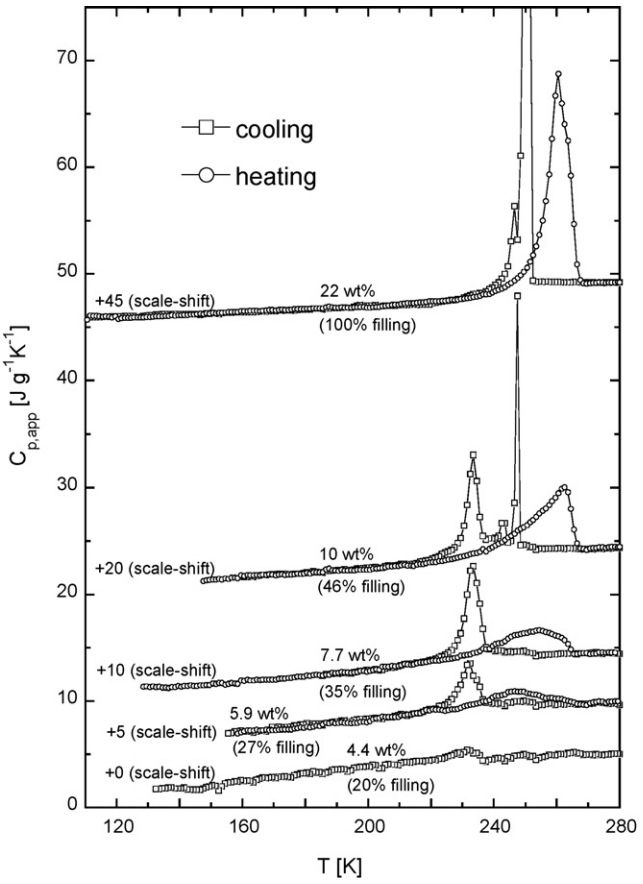

Fig. 3. The plots of $C_{p,app}$ for water in 4 nm pores of Vycor containing 4.4, 5.9, 7.7, 10 and 22 wt% water (20, 27, 35, 46 and 100% pore-filling). Measurements made during cooling the samples at 12 K/h from 280 to 110 K and then heating at the same rate after the precooled sample had been kept at 110 K for 1 h. The plots have been shifted upwards and the scale-shift is noted.

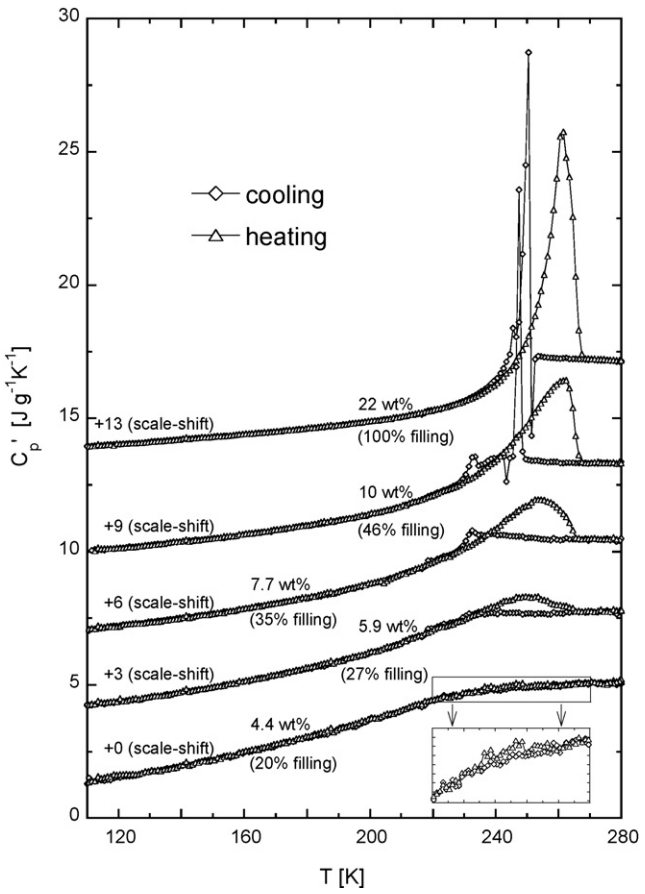

Fig. 4. The plots of C'_p for water in 4 nm pores of Vycor containing 4.4, 5.9, 7.7, 10 and 22 wt% water (20, 27, 35, 46 and 100% pore-filling). Insert shows a vertical scale enlargement of the 4.4 wt% pore-filling curves. Measurements made during cooling the samples at 12 K/h from 280 to 110 K and then heating at the same rate after the precooled sample had been kept at 110 K for 1 h. The plots have been shifted upwards and the scale-shift is noted.

peaks near 240 K on cooling at 5 K/min and one broad endotherm in the 260–270 K on heating. They also found an apparent T_g feature at T near 165 K. Finally they concluded that "The H-bond interaction of the interfacial water molecules with the numerous dangling OH groups (16 silanols/nm^2) at the Vycor surface supports the similarity (the value of T_g = 165 K in particular) between a water monolayer absorbed on Vycor and bulk water." The various arguments against the suggestions of T_g of 165 K for nanoconfined water and the observed calorimetric features of water in nanoconfinements have been discussed [1,20,21]. Arguments have also been given against the suggestion for T_g of 165 K for bulk water [22,23], which may be consulted for details. DSC studies of partially filled pores of silica have been reported also by Takamuku et al. [24]. They interpreted the data on the basis of results obtained from studies of the structural and dynamics properties. Zanotti et al. [19] have discussed already the limitations of that interpretation.

In these earlier studies, C_p and its change with T as well as with pore-filling was also separated from the thermal effects of freezing and melting. However, some of the earlier results differ from ours. The difference is partly attributable to the difference in concentration of water in Vycor or in silica samples in the respective studies, and partly to the procedure used for filling the pores and to the technique used for the measurements. A recent review [1] and two papers [20,21] have also shown that thermodynamic properties of water in nanoconfinement vary with the pore size in the matrix and the pore-size distribution.

4. Discussion

4.1. State of water in partially filled pores

In experiments intended to determine the energy of a water molecule [13], C'_p measured in real time during the course of transfer of water to 4 nm pores *via* the vapour phase [14] had shown that, after the bulk water available for transfer was exhausted, the pore water redistributed asymptotically with time. This minimized the net energy. Since our present experiments were performed on the samples of those experiments, water in the pores had already redistributed. To consider how water may be ultimately distributed in the partially filled pores, we first recall that some of the H_2O molecules form an uncrystallizable layer on the silica surface that is strongly bonded to the pore-wall. After that, there are two ways in which the remainder of the molecules may be present in the pores: (i) they may form concentric layers of hydrogen bonded structure, growing inwards radially as the pore-filling is increased, (ii) they may form clusters attached to the silica wall separated from each other, leaving parts of the volume unoccupied. Each of these would have a characteristic consequence for transformation of the state of water in the pores on cooling and on heating.

To consider the distribution of the 22 wt% water in Vycor, we recall that according to the manufacturer's data, the void space in Vycor 7930 is ~28% by volume, and dry Vycor's approximate density is 1.5 g/cm^3 (specific volume = 0.67 cm^3/g). This yields a maximum pore volume of ~0.19 cm^3/g of Vycor. By using the density of water

as 1 g/cm^3, we estimate that slightly more than 19 wt% water in Vycor would completely fill its pores. Any excess water would be outside the pores and would freeze on cooling, which would then melt on heating like bulk water at T near 273 K. In this study, we found no such melting endotherm for 22 wt% water content. This shows that for this amount, all water is contained in the pores. Two more effects need to be mentioned: Firstly, since there is distribution of pore size in the Vycor, our calculations of the total amount of water needed to cover the entire pore-wall and the amount needed to completely fill the channels may be approximate. As discussed earlier [7], this has little effect on our conclusions. Secondly, the possible solubility of silica in water, which was not considered by others, has been shown to be inconsequential [7].

Interactions at the silica–water interface also has an effect on hydrogen bond structure. Since the covalent bonds between the Si and O atoms near the surface are strained, the O atoms on the pore-wall are in a high-energy state. These may form hydrogen bonds with water by accepting a proton and thus form a hydrated layer on a pore's internal surface. Such hydrophilic effects have been referred to as the hydrated silica or –SiOH interactions. It has been accepted that their role is limited only to the first layer of H_2O molecules at the silica pore-wall. Thus, when an H_2O molecule is transferred to the nanopore *via* the vapour phase, it would initially go to the smallest pores in which the surface Si–O–Si bonds are highly distorted, because of relatively large surface–molecule interaction. Thereafter, further molecules would selectively go to successively larger pores if there were a distribution of pore size in Vycor. In this case, some of the wider pores may remain empty, if H_2O molecules were to reach those pores only *via* a (narrow and plugged) passage of the narrower pores. Consequently, complete pore-filling would either not be achieved or would be achieved only after slow diffusion of molecules out of the constricted passage into larger pores. Since transfer from a smaller pore's surface to a larger pore's surface would be endothermic (transfer of bulk water to pore water is exothermic), this latter process is energetically improbable, unless the entropy change is high enough to compensate for the enthalpy change and decreases the free energy.

NMR studies [25] in two silica matrices of MCMs (with cylindrical pores of uniform diameter or narrow distribution) have shown that the filling mechanism depends also upon the silica material. In the computer simulated distribution of H_2O molecules in nanopore channels [26,27], a radial heterogeneity of molecular distribution has been found, and it has been envisaged that ice-like structures form even in carbon nanotubes [28]. Gallo et al. [29] have performed molecular dynamics simulation of water confined in Vycor glass pores. A layer analysis of the site–site radial distribution functions gave evidence for the presence of two subsets of water molecules with different microscopic structure. Molecules in the inner layer next to the core were found to have the same structure as bulk water, and molecules close to the silica wall were found to be strongly influenced by the hydrophilic interactions with the wall and the structure contained distorted hydrogen bonds. They found that lowering of hydration has little effect on the structure of water in the outer layer. Although relevant, they do not have a significant consequence for our studies. It is also known that computer simulated results vary with the type of potential function used, and Puibasset and Pellenq [30] have stated that, "In the case of Vycor fully saturated with water, the oxygen–oxygen distribution function shows a higher structure than for bulk water, the contribution being probably mainly due to the contribution of water molecules close to the surface" [30]. (Higher structure means higher peak heights in the plot of the distribution function in their Fig. 3.) Some of these conclusions create an ambiguity in the usual discussion in which the nanopores are assumed to be filled from the pore-wall inwards. The filling may be radially uniform or else radially nonuniform as would occur when H_2O molecules form clusters attached to the pore-wall. On the basis of our finding, we regard the latter as a more probable occurrence.

4.2. Structural transformation on cooling and heating

To interpret our results in terms of structural transformation of water in 4 nm pores, we adapt some of the arguments given by Mallamace et al. [31] and by one of us in a paper in this issue of the journal [1]. An H_2O molecule has an average volume of ~30 Å^3 (= $18/6.03 \times 10^{23}$). The effective diameter of its circumscribed sphere is therefore 0.38 nm. If the uncrystallizable H_2O nanoshell bonded to the silica surface were one-molecule thick, there will be eight H_2O molecules (= (4.0/0.38) – 2) left to form a nanocore of ~3.2 nm diameter in a 4 nm pore. If it were two-molecule thick, there will be six H_2O molecules (= (4/0.38)– 4) left to form the nanocore of ~2.5 nm diameter. The unit cell dimensions of hexagonal ice (space group $P6_3/mmc$, containing four H_2O) are, $a = b = 0.448$ nm and $c = 0.731$ nm, and of cubic ice (space group $\overline{4}3m$, containing eight H_2O) are $a = 0.638$ nm. Therefore, for forming one unit cell of the structure of these ices, a nanocore of at least ~0.76 nm (two molecule) diameter is required. For nucleation of the ices a volume containing a much larger number of molecules would be needed.

We begin by considering the transformation in 4.4 wt% pore water (20% filling). According to the manufacturer, the surface area of the pores is 250 m^2/g. Since the diameter of a water molecule is 0.386 nm, a dense-packed one-molecule thick layer of H_2O next to the pore-wall would consist of 16.8×10^{20} H_2O molecules, which amounts to 50.4 mg (2.79 mM) of water per g of Vycor or to ~5 wt% of water. If a two-molecule thick layer were to form, this amount would be ~10 wt% water. Any amount less than 5 wt% will not completely cover the pore-wall, and any amount more than that will either form a second layer of H_2O molecules or else form molecular clusters within the pores. Therefore, according to the above-given distribution, the 4.4 wt% pore water in Vycor would not be enough to form one-molecule thick layer which does not crystallize on cooling, as discussed above. However, the $C_{p,\mathrm{app}}$ against T plot for 4.4 wt% pore water in Fig. 3 shows a tiny exothermic peak at ~233 K on cooling. The C'_p against T plot for this sample in Fig. 4 shows only a change of slope at T near 245 K. Moreover, the C'_p data obtained for cooling slightly differ from the C'_p data obtained on heating, as seen in Fig. 4 insert. This is an indication, though marginal, that in the sample containing 4.4 wt% pore water, not all the H_2O forms an uncrystallizable nanoshell bonded to silica. It is conceivable that a small amount of H_2O forms clusters on the silica wall that transform to a low entropy structure (partially ordered H-bond network) of water molecules on cooling. If this has occured then the endotherm due to the reverse transformation on heating has so broadened that it is undetectable within the sensitivity of our measurements.

The $C_{p,\mathrm{app}}$ against T plots of the 5.9 and 7.7 wt% pore water in Fig. 3 show a sharp peak on cooling and a broad peak on heating, with a hysteresis of 16 and 25 K, respectively. The corresponding plots of C'_p in Fig. 4 show similar features on cooling and heating. In these pores, the amount of water is more than the amount needed to form a one-molecule thick layer. The extra amount may form a part of the second layer of H_2O hydrogen bonded to the molecules in the first layer. If that occurred, at most two H_2O molecules would be available to transform to ice or to another low entropy structure. Since one ice unit cell contains at least six H_2O molecules, ice would form only if H_2O molecules formed clusters attached to the uncrystallizable monolayer bonded to the siloxane on the silica surface of the pore. The sharpness of the exothermic peak on cooling for 5.9 and 7.7 wt% pore water does indicate the rapidity of crystallization similar to that observed on crystallization of supercooled bulk water to ice, and the broadness of the endothermic peak on heating indicates a gradual transformation without a distinct melting point.

The higher amount of 10 wt% pore water (46% pore-filling) is also enough to form one-molecule thick, uncrystallizable nonoshell with an additional large number of H_2O hydrogen bonded to this shell. The thickness of the extra layers for the 46% filling is large enough to form hexagonal and/or cubic ice unit cells, but not enough to show a diffraction pattern. Alternatively, some H_2O for this filling may exist as clusters and some may fill the pores. Following the arguments for the exotherm at 233 K and the endotherm in the 245–265 K range found for lower amounts of pore water, we consider that the 233 K exothermic peak is due to the transformation of H_2O clusters, and the 247–250 K peak due to crystallization of the water in the filled pores forming regions in which several unit cells of the ices can form. Thus, we attribute the high temperature peak to crystallization in the filled regions in the pores and the 233 K peak to crystallization of clusters separated from the filled regions.

As described above, for the 22 wt% pore water (100% filling) there will be eight (linearly arranged) H_2O molecules (= (4.0/0.38) − 2) left to form a nanocore of ∼3.2 nm diameter in the 4 nm diameter pore of Vycor. Thus, all water may crystallize in a narrow range showing only one prominent exothermic peak, as is observed in Figs. 1 and 3. The solid formed on cooling may on heating melt with an equally prominent endothermic peak at $T < 273$ K, according to the Gibbs–Thomson equation. Unlike the unfilled pores, there are no clusters of H_2O molecules that would freeze to ice or to a low energy structure at 233 K.

We also consider another aspect of this interpretation. It is believed that the density of bulk water approaches the density of ice at $T < 225$ K, which may not be the case for nanopore water. However, if the volume increase on crystallization in 100% filled pores were the same as for bulk water, it would produce a maximum of ∼2 kbar pressure in a hermetically sealed pore on crystallization at ∼251 K. This may expel some of the water from the open and/or loosely plugged pores. In the latter case, the expulsion rate of water would determine the growth rate of ice in the sample. In any case, the ice-like structure formed along the pore axis would remain exceptionally small even if pressure persisted in the pore.

Finally we interpret the broadness of the endothermic peak on melting in relation to the exothermic peak on crystallization. As discussed earlier [1,7], the broadness of the peak indicates a gradual transformation of ice-like structures to the "melt state" in a temperature range in which ice and the "melt" coexist. The coexistence equilibrium arises when change in the Gibbs energy per unit volume [32] becomes equal to the opposite change in the interfacial energy associated with the grain junctions and grain boundaries. Premelting of ice associated with this effect has been found in a study of micrograin size ice samples [33].

As found in an earlier study, in which cooling was limited to 233 K [7], nanoconfined water in this study shows a thermal hysteresis of the transformation. A thermal hysteresis has also been observed by NMR cryoporometry studies which have shown the hysteresis to vary also with the surface to volume ratio of the pores and with the curvature of the pore surface [34]. Moreover, X-ray diffraction studies of water in 3.5 nm size pores have shown a continuous transition between the liquid and crystalline state that precedes the first order freezing transition of pore water [35].

To investigate the nature of crystallization as evident from exothermic peaks, we performed additional experiments. The sample containing 10 wt% pore water was cooled from 280 to 240 K at 12 K/h rate, a region in which crystallization occurs only in the 250 K range. By using this temperature range, crystallization that occurs at 233 K could be prevented. The data are plotted in Fig. 5A, which shows that one large and one very small exothermic peak at 248 and 242 K, respectively. Thereafter, the sample was kept at 240 K for 15 min and then heated to 280 K at 12 K/h rate. The data plotted in Fig. 5B show one endothermic peak at ∼262 K. The data for

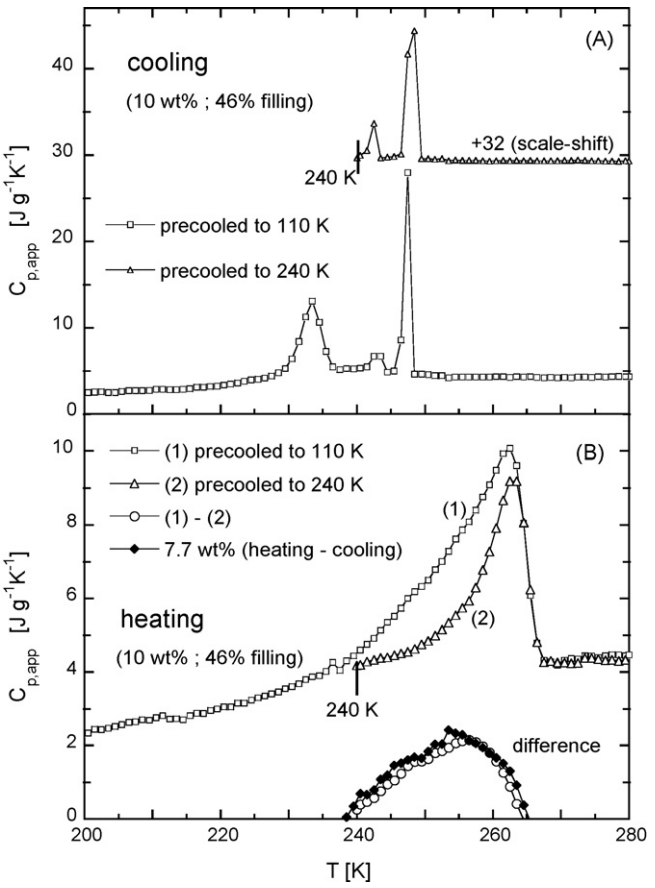

Fig. 5. The plots of $C_{p,app}$ for water in 4 nm pores of Vycor containing 10 wt% water (46% filling). (A) Measurements made during cooling the samples at 12 K/h from 280 to 240 K (top plot), and from 280 to 110 K (bottom plot). (B) Measurements made on heating to 280 K the sample that had been precooled to 240 K and kept at 240 K for 15 min. Also shown is the corresponding plot for the sample precooled to 110 K. The difference between the $C_{p,app}$ of the two plots is provided together with the difference between heating and cooling $C_{p,app}$ data observed for the 7.7 wt% pore water sample shown in Fig. 3, for which only one exothermic peak at ∼233 K was observed on cooling.

10 wt% pore water taken from Figs. 1 and 2 are replotted in Fig. 5A and B. It is evident in the plots that when the sample has been precooled to 110 K it still shows an endothermic peak at ∼262 K, but the peak is broadened at the low-temperature side, indicating a possible overlap of two endothermic peaks. This means that the state that had formed at T near ∼233 K on cooling to 110 K melts on heating at a lower T than the state that had formed on cooling only to 240 K. To further elaborate, we determined the difference between the $C_{p,app}$ measured on heating the sample that had been precooled to 110 K (curve 1, Fig. 5B) and the $C_{p,app}$ measured on heating the sample that had been precooled to 240 K (curve 2, Fig. 5B). This difference is plotted (circles) also in Fig. 5B. It shows a broad peak at 255 K, which agrees with the difference (filled diamonds) between the $C_{p,app}$ data observed for heating and cooling of the 7.7 wt% pore water sample shown in Fig. 3, for which only one exothermic peak at ∼233 K was observed on cooling. We conclude that there are not just two crystallization regions; there are also two melting regions, and the melting range is much broader than the crystallization range.

At first sight it seems that our data could provide a quantitative analysis of the change in the vibrational contribution to the specific heat of supercooled water and ice from bulk states to the nanoconfined states. Unfortunately, this contribution has not been experimentally determined for supercooled water. For ice, the measured C_p is entirely vibrational. A comparison of its C_p with the value determined here may indicate the crystalline state of water

in Vycor. But the differences between the respective C_p values of cubic, hexagonal and amorphous ices are too small to be distinguishable within the sensitivity of our measurements. Briefly, it has been found that there is less than 1% difference between the C_p of hexagonal ice [36] and cubic ice [37,38]. Also, C_p of amorphous ice [37] and the two crystalline ices are within 1%. When hexagonal ice becomes proton-ordered to ice XI [39,40] and its entropy decreases, the small change in C_p is also well within 1%. The specific heat of pore ice in Vycor here has been determined by (a) subtracting the mass of dry Vycor from the sample's mass to estimate the total amount of water in the sample, (b) subtracting the measured C_p in J/(g K) of the dry Vycor from the measured C_p of the sample per g of pore water. These steps add error to the C_p estimate of pore ice by at least 2%. Therefore, whatever state of ice was formed in the nanopores, it could not be distinguished on the basis of our C_p data.

4.3. Pore-filling effects and pore-size effects

Oguni et al. [11] have studied $C_{p,\mathrm{app}}$ of water in pore sizes 1.1–52 nm of various silica gels by adiabatic calorimetry. The sample pores were 100% filled with water and the data were obtained only on heating. The results were reported as plots of $C_{p,\mathrm{app}}$ against T. In their Figs. 4 and 5, they showed that for 100% filling by both H_2O and D_2O, the onset temperature of $C_{p,\mathrm{app}}$ rise for small size pores was low, and the plots had a broad shape. As the pore size was increased, still with 100% pre-filling, the onset temperature of $C_{p,\mathrm{app}}$ rise increased, the plots became narrower and for 52 nm pores, $C_{p,\mathrm{app}}$ rose sharply as the ice melted at T close to 260 K. To compare these effects against our findings for experiments in which pore-filling has been varied, we have replotted the $C_{p,\mathrm{app}}$ data measured during heating for the various pore-fillings in Fig. 6. The onset temperature for the melting endotherm for the lowest pore-filling (4.4 wt%) cannot be estimated, as the endotherm is too broad and therefore, we disregard it here. For higher pore-filling, the onset temperature increases with increase in the pore-filling. The plots are broader for 20% pore-filling and become narrower as the pores are filled to 100%. (The apparent oscillations in $C_{p,\mathrm{app}}$ seen for 5.9 wt% are partly due to fluctuation of the baseline instability amplified by the large subtraction of $C_{p,\mathrm{app}}$ of dry Vycor needed to obtain these values. Note that such fluctuations do not appear in the C_p' plots shown in Fig. 2.)

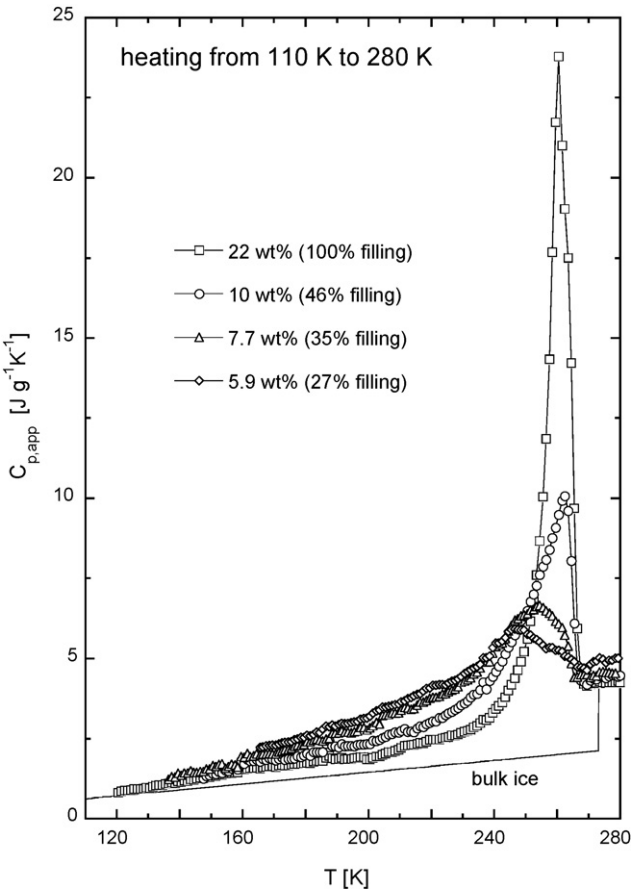

Fig. 6. The plots of $C_{p,\mathrm{app}}$ for water in 4 nm pores of Vycor containing 5.9, 7.7, 10 and 22 wt% water (27, 35, 46 and 100% pore-filling) as measured during the heating from 110 to 280 K at 12 K/h. The dashed line is for ice. The samples were precooled to 110 K at 12 K/h and kept for 1 h before heating. The errors caused for the 4.4 wt% were too large for inclusion here. The plots resemble those in Figs. 4 and 5 of Ref. [11], a study in which the pore size was increased from 1.1 to 52 nm and the filling was 100%.

The similarity between the plots in Fig. 6 and the plots in Figs. 3 and 4 in Oguni et al.'s study [11] is remarkable. This indicates that the change in the onset temperature and shape of the "melting" transformation endotherm obtained by varying the pore size with 100% filling can be achieved also by partially filling the pores of a given size. This means that on cooling, the manner in which crystallization of water changes depends upon the distribution of water in the pores. There is also a difference between these studies and Oguni et al.'s [11]. Our studies were performed during both the cooling and heating and theirs were necessarily limited to measurements on heating as they used adiabatic calorimetry and therefore it is not clear whether Oguni et al. [11] could have also observed several exothermic peaks due to crystallization on cooling of the pore water. Nevertheless, the observations here suggest that it is necessary to perform $C_{p,\mathrm{app}}$ measurements during both cooling and heating for the purpose of revealing the nature of transformations in the pore water.

5. Conclusions

The exothermic and endothermic features of water in 4 nm pores show a transformation that varies with the amount of pore water, i.e., the extent of filling of the pores. For a given amount of pore water, the distribution of water is envisaged (i) as uncrystallizable layer of H_2O bonded to the silica surface, (ii) as H_2O clusters only partially filling the pores, and (iii) as regions of hydrogen bonded and packed H_2O molecules in the pores. When the total amount of water is comparable to the amount needed to form an uncrystallizable monolayer attached to the silica wall, some H_2O still form a cluster that may crystallize to an ice or else to a low entropy structure on cooling, with an exothermic peak at ~233 K. As the filling is increased, a larger population of H_2O molecules aggregate to form clusters at random sites inside the pore and the crystallization peak at ~233 K grows. On heating, an endothermic peak due to melting appears at ~255 K. For 46% filling some of the water forms H_2O clusters and some fills certain regions of the pores. A preliminary study of 100% water-filled pores of MCM has shown two melting endotherms which may indicate lack of radially symmetrical layer of water in these pores. However, the pore size is less than 3 nm. Studies in larger pore-size MCMs would be needed to examine this.

Freezing of water in the completely filled pores produces a prominent exothermic peak at 250 K and indicates crystallization of the packed regions in the pores. Heating melts the state of solid formed in both stages of crystallization and broadens the endotherm. For 100% pore-filling, there are no H_2O clusters and therefore only the prominent exothermic peak due to crystallization in the packed pores is observed. The assumption of a radially symmetrical layer of free H_2O molecules seems to be inconsistent with the observed crystallization of water in partially filled pores. Rather, H_2O molecules would likely be clustered in the pores in

addition to the partial covering by an uncrystallizable layer on the pore-wall.

A separate study of cooling to different temperatures and thereafter heating confirms the occurrence of a two-stage crystallization and two-stage melting in the partially filled pores, but the two melting endotherms overlap, thereby broadening the endothermic peak on its low-temperature side.

The change in the shape of the endotherms, i.e., of $C_{p,\mathrm{app}}$ and C_p' plots against T, and the increase in the onset temperature of the melting endotherms on increase in the pore-filling to 100% are remarkably similar to the corresponding change and related effect observed on increasing the 100% filled pore size. Studies of structural transformation of water in the pores is more appropriately followed by both cooling and heating and measuring in each case both the $C_{p,\mathrm{app}}$ and C_p'.

Acknowledgement

G.P.J. would like to thank the IPCF-CNR, Pisa, for their hospitality during the period of his stay for these studies.

References

[1] G.P. Johari, Thermochim. Acta (2009), doi:10.1016/j.tca.2009.02.021.
[2] J. Dore, Chem. Phys. 258 (2000) 327.
[3] B. Webber, J.C. Dore, J. Phys.: Condens. Matter 16 (2004) S5449.
[4] K. Morishige, H. Uematsu, J. Chem. Phys. 122 (2005) 044711.
[5] K. Morishige, H. Iwasaki, Langmuir 19 (2003) 2808.
[6] J. Rault, R. Neffati, P. Judeinstein, Eur. Phys. J. B 36 (2003) 627.
[7] E. Tombari, G. Salvetti, C. Ferrari, G.P. Johari, J. Chem. Phys. 122 (2005) 104712 (Units of H and G in Figs. 3(b) and 4(b) should read kJ/mol).
[8] S. Kittaka, S. Ishimaru, M. Kuranishi, T. Matsuda, T. Yamaguchi, Phys. Chem. Chem. Phys. 8 (2006) 3223.
[9] S. Jähnert, F. Vaca Chávez, G.E. Schaumann, A. Schreiber, M. Schönhoff, G.H. Findenegg, Phys. Chem. Chem. Phys. 10 (2008) 6039.
[10] S. Maruyama, K. Wakabayashi, M. Oguni, AIP Conf. Proc. 708 (2004) 675.
[11] M. Oguni, S. Maruyama, K. Wakabayashi, A. Nagoe, Chem. Asian J. 2 (2007) 514.
[12] A. Fouzri, R. Dorbez-Sridi, M.M. Oumezzine, J. Chem. Phys. 116 (2002) 791.
[13] E. Tombari, G. Salvetti, C. Ferrari, G.P. Johari, Phys. Chem. Chem. Phys. 7 (2005) 3407.
[14] E. Tombari, G. Salvetti, C. Ferrari, G.P. Johari, J. Chem. Phys. 123 (2005) 214706.
[15] G. Salvetti, C. Cardelli, C. Ferrari, E. Tombari, Thermochim. Acta 364 (2000) 11.
[16] G. Salvetti, E. Tombari, L. Mikheeva, G.P. Johari, J. Phys. Chem. B 106 (2002) 6081.
[17] M. Merzlyakov, C. Schick, Thermochim. Acta 330 (1999) 55.
[18] M.-C. Bellissent-Funel, J. Lal, L. Bosio, J. Chem. Phys. 98 (1993) 4246.
[19] J.-M. Zanotti, M.-C. Bellissent-Funel, S.H. Chen, Europhys. Lett. 71 (2005) 91.
[20] G.P. Johari, E. Tombari, G. Salvetti, F. Mallamace, J. Chem. Phys. 130 (2009) 126102.
[21] G.P. Johari, J. Chem. Phys. 130 (2009) 124518.
[22] G.P. Johari, J. Chem. Phys. 116 (2002) 8067.
[23] G.P. Johari, J. Chem. Phys. 119 (2003) 2936.
[24] T. Takamuku, M. Yamagami, H. Wakita, T. Yamaguchi, J. Phys. Chem. B 101 (1997) 5730.
[25] B. Grünberg, T. Emmler, E. Gedat, I. Shenderovich, G.H. Findenegg, H.-H. Limbach, G. Buntkowsky, Chem. Eur. J. 10 (2004) 5689.
[26] I. Brovchenko, A. Geiger, A. Oleinikova, Phys. Chem. Chem. Phys. 6 (2004) 829.
[27] I. Brovchenko, A. Geiger, A. Oleinikova, D. Paschek, Eur. Phys. J. E 12 (2003) 69.
[28] J. Wang, Y. Zhu, J. Zhou, X.-H. Lu, Phys. Chem. Chem. Phys. 6 (2004) 829.
[29] P. Gallo, M.A. Ricci, M. Rovere, J. Chem. Phys. 116 (2002) 342.
[30] J. Puibasset, R.J.-M. Pellenq, Eur. Phys. J. E 12 (2003) 67.
[31] F. Mallamace, E. Tombari, G. Salvetti, G.P. Johari, arXiv: 0806.4775vi [cond-mat.soft] (2008).
[32] G.P. Johari, W. Pascheto, S.J. Jones, J. Chem. Phys. 100 (1994) 4548.
[33] G. Salvetti, E. Tombari, G.P. Johari, J. Chem. Phys. 102 (1995) 4987.
[34] O. Petrov, I. Furó, Phys. Rev. E 73 (2006) 011608.
[35] K. Morishige, K. Kawano, J. Chem. Phys. 110 (1999) 4867.
[36] O. Haida, T. Matsuo, H. Suga, S. Seki, J. Chem. Thermodyn. 6 (1974) 815.
[37] M. Sugaseki, H. Suga, M. Seki, Bull. Chem. Soc. Jpn. 41 (1968) 2591.
[38] O. Yamamuro, M. Oguni, T. Matsuo, H. Suga, Phys. Chem. Solids 48 (1987) 935.
[39] O. Yamamuro, M. Oguni, T. Matsuo, H. Suga, J. Chem. Phys. 86 (1987) 5137.
[40] T. Matsuo, H. Suga, J. Phys. Colloques 48 (1987) C1-477.